# Complex Permittivity and Permeability Measurements and Finite-Difference Time-Domain Simulation of Ferrite Materials

Jianfeng Xu, *Member, IEEE*, Marina Y. Koledintseva, *Senior Member, IEEE*, Yaojiang Zhang, *Member, IEEE*, Yongxue He, Bill Matlin, Richard E. DuBroff, *Senior Member, IEEE*, James L. Drewniak, *Fellow, IEEE*, and Jianmin Zhang, *Senior Member, IEEE*

***Abstract*—A methodology to efficiently design products based on magneto-dielectric (ferrite) materials with desirable frequency responses that satisfy electromagnetic compatibility and signal integrity requirements over RF and microwave bands is presented here. This methodology is based on an analytical model of a composite magneto-dielectric material with both frequency-dispersive permittivity and permeability. A procedure for extracting complex permittivity and permeability of materials from experimental data is based on transmission line measurements. The genetic algorithm is applied for approximating both permittivity and permeability of materials by series of Debye frequency dependencies, so that they are represented as "double-Debye materials" (DDM). The DDM is incorporated in the finite-difference time-domain numerical codes by the auxiliary differential equation approach.**

***Index Terms*—Complex permeability, cylindrical core, Debye frequency dependence, finite-difference time-domain (FDTD) modeling, genetic algorithm (GA), permittivity.**

## I. Introduction

FERRITES are nonconducting ferrimagnetic materials that are widely used for solving numerous electromagnetic compatibility (EMC) and signal integrity (SI) problems. For example, the design of nonconductive absorbing shielding enclosures, coatings, and gaskets for improving immunity of electronic equipment is important from the point of view of eliminating possible surface currents as sources of undesirable emissions. Combining dielectric or conducting inclusions with ferrite particles in a composite absorbing material may substantially increase the absorption level in the frequency range of interest. Sleeves or clamps, made of bulk-sintered ferrites, are widely used as electromagnetic interference suppressing filters on cables. Ferrite beads are used as lumped elements on printed circuit boards for SI purposes.

This paper is aimed at the development of an efficient and systematic methodology for analysis and design with magneto-dielectric materials and ferrite components for EMC and SI solutions in electronic designs. The methodology includes the extraction of the complex permittivity and permeability of magneto-dielectric (ferrite) materials from measurements, and an efficient numerical simulation approach, incorporating frequency-dispersive magnetic and dielectric materials, and allowing for efficient and accurate simulation of complex geometries containing these materials.

The intrinsic complex permeability and permittivity are critical parameters for the design optimization of devices based on soft spinel ferrites, such as Ni-Zn, Mn-Zn, or others, as well as wideband examination of their performance, especially at higher frequencies (up to GHz range) [1]–[3]. Characterization of high-frequency permeability and permittivity of materials can be done by various approaches [4]. The most well known are:

1) the bridge method containing lumped elements—this method is applicable only for frequencies below 1 MHz [5];
2) quasi-optical methods based on measuring phase velocity and attenuation of plane electromagnetic waves in the material under study—these methods can be applied in cm and mm wavebands [6], [7];
3) cavity methods using small samples under test, based on perturbations in the Q-factor and resonance frequency measurements under loaded and unloaded conditions [4];
4) transmission line (waveguide) techniques with standing waves, where the end of the line is shorted, and a thin slab under test is placed in a magnetic field node for permittivity measurements, and in an electric field node for permeability measurements; these methods are based on the variation of standing wave ratio and shift of electric or magnetic field minima, when the sample under test is used [5], [8]; and
5) transmission line (waveguide) techniques with propagating waves—based on measuring the transmission coefficient in two independent measurements, since both dispersive and dissipative parts of complex permeability (or permittivity) must be determined.

Manuscript received June 14, 2009; revised January 19, 2010 and April 13, 2010; accepted April 15, 2010. Date of publication July 12, 2010; date of current version November 17, 2010.

J. Xu, M. Y. Koledinstseva, R. E. Dubroff, and J. L. Drewniak are with Missouri University of Science and Technology, Rolla, MO 65409 USA (e-mail: jianfeng@mst.edu; marinak@mst.edu; drewniak@mst.edu; red@mst.edu).

Y. Zhang was with the Institute of High Performance Computing, Singapore 138632. He is now with the Electromagnetic Compatibility Laboratory, Missouri University of Science and Technology, Rolla, MO 65409 USA.

Y. He and B. Matlin are with Laird Technologies, Chattanooga, TN 37407 USA (e-mail: yongxue.he@lairdtech.com; bill.matlin@lairdtech.com).

J. Zhang is with the Cisco System, Inc., San Jose, CA 95134 USA (e-mail: jianmin@cisco.com).

Color versions of one or more of the figures in this paper are available online at http://ieeexplore.ieee.org.

Digital Object Identifier 10.1109/TEMC.2010.2050693

The easiest way in the latter method is to measure phase shift and attenuation in a long ferrite sample completely filling a waveguide cross section [9]. However, to separate dielectric and magnetic characteristics, the corresponding electromagnetic boundary problem must be solved [10].

There are modern automated methods of extraction of complex permittivity and permeability of dielectric/magnetic bulk materials and thin films. These methods are based on transmission/reflection or short-circuit line broad-band measurements. To obtain $S$-parameter characterization, network analyzers [11]–[14], or time-domain reflectometers are commonly used [15]. The measurements can be done in waveguides [11], coaxial lines [12], [16], and stripline geometries [17]–[19].

The present method is based on measuring the complex characteristic impedance ($Z_w$) and propagation constant ($\gamma$). The method utilizes an impedance analyzer (IA) and is applied to structures with a single-mode propagating (e.g., TEM). Here, the two independent measurements carried out are for extracting complex $\mu$ and $\varepsilon$ and are with open and short terminations at the end of the test sample. This is based on the well-known fact that the characteristic impedance of the line can be obtained through the input impedances in open and shorted cases [20].

As soon as the parameters of the material under test are extracted, the corresponding frequency dependencies can be curve fitted by a series of rational fractional terms, which are convenient for further numerical modeling and satisfy the Kramers–Kronig causality relations [21]. In the simplest case of comparatively smooth frequency dependencies without pronounced resonance effects, these are the Debye-like terms with poles of the first order [22]. Then desirable structures with these extracted permittivity and permeability characteristics can be modeled numerically, and the resulting structures can be analyzed and optimized at the design stage.

The novel methodology of analysis and design of ferrite chokes and cores is discussed in Section II of the present paper. This approach is based on a combination of 1) a simple technique for measuring complex-shaped frequency characteristics (both $\mu$ and $\varepsilon$) of ferrite materials; 2) application of an optimization technique such as a genetic algorithm (GA) curve fitting of the resultant mu and epsilon frequency dependencies by sums of Debye-like terms; and 3) incorporation of these Debye terms in numerical finite-difference time-domain (FDTD) codes that provide wideband responses of complex ferrite-containing structures due to the nature of time-domain codes. The material parameters (permittivity and permeability) are extracted using specially made hollow ferrite cylindrical coaxial structures and analytical expressions. This is done to get frequency dependencies of permittivity and permeability of the materials that could be used in different products made of the same ferrite material. Comparison between simulations and measurements are presented in Section III. The correctness of our numerical EZ-FDTD codes with incorporated material frequency characteristics of ferrite is validated by "sanity check" done through comparing the measured input impedance with the EZ-FDTD-modeled input impedance. Then the extracted material parameters are used for modeling other ferrite structures (common-mode chokes), and the results of modeling are compared with the corresponding experimental results. The conclusions are summarized in Section IV of the paper. The presented approach allows for efficiently running numerical experiments and parametrically varying input material/geometry parameters until the desired frequency characteristics of ferrite-containing structures are achieved. This methodology would provide ferrite manufacturers with useful data how to change contents of engineered materials to get the products and devices with the best possible functional possibilities and may be a part of a design cycle for industry.

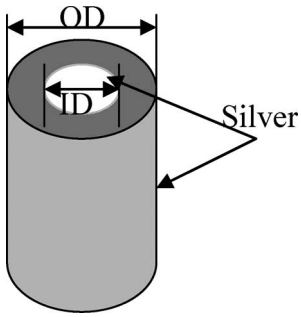


Fig. 1. Ferrite core coated with silver.

## II. Methodology

The methodology for analysis and design of ferrite components is presented here. It includes the measurement setup and technique, an extraction procedure, curve fitting, and incorporation of the frequency-dependent parameters into the FDTD numerical method.

### A. Complex Permittivity and Permeability Measurement

Waveguiding structures with a well-contained electromagnetic field within a transmission line section under test are suitable for measuring parameters of magneto-dielectric (ferrite) materials. The important condition is that the cross section of the line is completely and homogeneously filled with the material under test and must have a translationally invariant cross section. These measurements can be comparatively wideband, if there is a single-mode propagation of electromagnetic wave on the line over the frequency range of interest, e.g., TEM wave. TEM mode propagation is favorable for measurements on magnetic materials. The key point is that the magnetic field lines would form closed loops inside the material under test, so that the demagnetization effects would be minimized, and the material would fully respond to the incident magnetic field. This means that it is necessary to specially manufacture test samples of materials to form a transmission line. Two geometries for measuring material parameters of ferrite samples are coaxial and stripline structures.

In the present study, a ferrite cylindrical core with silver-plated internal and external surfaces, as is shown in Fig. 1, has been used for the tests. The conductor inner diameter and outer diameter are 7.2 and 14 mm, respectively. The length $L$ of the core is 28 mm.

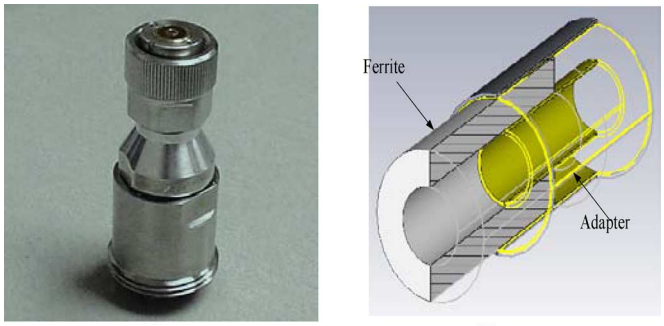


Fig. 2. (a) Precision adapter. (b) mechanical connection.

The electromagnetic parameters of the silver-coated ferrite core, which is the device under test (DUT), have been measured using an IA HP4291 A. The DUT is connected to a specially designed precision adapter, as shown in Fig. 2(a) and (b). The operating frequency range for this setup was from 10 to 500 MHz. The upper frequency of this range is limited by increasing with the frequency loss in ferrite material. At frequencies close to 500 MHz, the amplitude of the wave reaching the end of the ferrite will be comparable to the noise level. Permeability and permittivity as functions of frequency are determined from the characteristic impedance $Z_w$ and propagation constant $\gamma$ through the input impedance measurements in short-circuit and open-circuit conditions as

$$Z_w = \sqrt{Z_{\text{short}} Z_{\text{open}}} \tag{1}$$

and

$$\tanh(\gamma l) = \sqrt{\frac{Z_{\text{short}}}{Z_{\text{open}}}} \tag{2}$$

where $l$ is the length of the transmission line sample. In the short-circuit case, the far end of the DUT is completely coated with silver, while in the open-circuit case, the silver coating is removed.

### B. Extraction of the Constitutive Parameters

A seemingly simple way to extract material characteristics of magneto-dielectric material filling a single-mode (TEM) transmission line from the measured characteristic impedance on the line $Z_w$ and propagation constant $\gamma$ is to get corresponding $R$, $L$, $G$, and $C$ per-unit-length parameters of the line from solving the system of equations

$$\begin{cases} \dfrac{\gamma}{Z_w} = G + j\omega C \\ \gamma Z_w = R + j\omega L. \end{cases} \tag{3}$$

Then an appropriate transmission line model is needed to relate complex permittivity and permeability with these extracted $R$, $L$, $G$, and $C$ parameters. This approach was applied, e.g., in [23] to extract complex permittivity of microstrip substrates with comparatively low-dielectric constant and dissipation factor. However, even for dielectrics with low loss and hence low frequency dispersion, there is a serious problem of separating dielectric loss from conductor loss, i.e., telling apart dissipative parameters $R$ and $G$, as well as contributions of reactive parameters $L$ and $C$. To do this, not only appropriate transmission line model is needed, but also accurate geometrical data of the line, and some *a priori* information on the dielectric properties behavior. The problem becomes very complicated, if surface roughness on the conductor is substantial, and ignoring it at higher frequencies (above a few GHz) might lead to substantial lumping of $R$ contribution to $G$, and $L$ to $C$, and vice versa.

In the case of lossy and highly dispersive materials, like ferrites, this problem becomes even more challenging. For this reason, in this paper, it is proposed to avoid intermediate step of getting $R$, $L$, $G$, and $C$ parameters, which may lead to additional errors, but directly split real and imaginary parts (or amplitude and phases, which is mathematically equivalent) in the measured $Z_w$ and $\gamma$ in the frequency range of interest, and then get complex permittivity and permeability.

Let us represent the complex characteristic impedance of the transmission line with a ferrite as

$$Z_w = R_w + jX_w. \tag{4}$$

On the other hand, the characteristic impedance can be expressed through the material parameters, since there is only the TEM mode propagating on this transmission line, as

$$Z_w = Z_0 \sqrt{\frac{\tilde{\mu}_r(\omega)}{\tilde{\varepsilon}_r(\omega)}} \tag{5}$$

where $\tilde{\mu}_r(\omega)$ and $\tilde{\varepsilon}_r(\omega)$ are, respectively, the unknown complex relative permeability and permittivity of the material under test, and $Z_0$ is the characteristic impedance of the empty (air-filled) transmission line, related to only to its geometry factor.

The complex propagation constant

$$\gamma = \alpha + j\beta \tag{6}$$

with attenuation constant $\alpha$ and phase constant $\beta$ can also be represented through the material parameters of ferrite filling in the transmission line as

$$\gamma = j\frac{\omega}{c}\sqrt{\tilde{\mu}_r \tilde{\varepsilon}_r} \tag{7}$$

where $c = 1/\sqrt{\mu_0 \varepsilon_0}$ is the speed of light in free space and $\omega = 2\pi f$ is the angular frequency.

Complex permittivity and permeability can be obtained through the system of four equations with four unknowns. This is done below in the general form for any line with single-mode TEM (or quasi-TEM) propagation, such as a coaxial line, a stripline, or a microstrip line.

Complex permittivity and permeability can be represented through their magnitudes and arguments, related to loss tangents, using Euler's representation as

$$\tilde{\varepsilon}_r = |\varepsilon_r| \exp(-j\delta_e) \tag{8}$$

and

$$\tilde{\mu}_r = |\mu_r| \exp(-j\delta_m). \tag{9}$$

Then the complex propagation constant can be written as

$$\gamma = \frac{\omega}{c}\sqrt{|\mu_r|\,|\varepsilon_r|}\exp\left(-j\left(\frac{\delta_m}{2}+\frac{\delta_e}{2}-\frac{\pi}{2}\right)\right) \tag{10}$$

and the complex characteristic impedance can be written as

$$Z_w = Z_0\sqrt{\frac{|\mu_r|}{|\varepsilon_r|}}\exp\left(-j\left(\frac{\delta_m}{2}-\frac{\delta_e}{2}\right)\right). \tag{11}$$

Separating real and imaginary parts of $\gamma = \alpha + j\beta$ in (9) gives

$$\alpha = \frac{\omega}{c}\sqrt{|\mu_r|\,|\varepsilon_r|}\sin\left(\frac{\delta_m}{2}+\frac{\delta_e}{2}\right) \tag{12}$$

and

$$\beta = \frac{\omega}{c}\sqrt{|\mu_r|\,|\varepsilon_r|}\cos\left(\frac{\delta_m}{2}+\frac{\delta_e}{2}\right). \tag{13}$$

Separating real and imaginary parts in (11) gives

$$R_w = Z_0\sqrt{\frac{|\mu_r|}{|\varepsilon_r|}}\cos\left(\frac{\delta_e}{2}-\frac{\delta_m}{2}\right) \tag{14}$$

and

$$X_w = Z_0\sqrt{\frac{|\mu_r|}{|\varepsilon_r|}}\sin\left(\frac{\delta_e}{2}-\frac{\delta_m}{2}\right). \tag{15}$$

Thus there is a system of four equations (12)–(15) with respect to four unknowns—$\{|\mu_r|, |\varepsilon_r|, \delta_m, \delta_e\}$. In this system, the $\alpha, \beta, R_w, X_w$ parameters are considered to be known, since they are directly obtained from measurements of input impedances in the short- and open-circuit cases. Solving this system of equations, after some algebraic transformations, gives

$$\varepsilon_r' = Z_0\frac{c}{\omega}\frac{R_w\beta - X_w\alpha}{R_w^2+X_w^2} \tag{16}$$

$$\varepsilon_r'' = Z_0\frac{c}{\omega}\frac{R_w\alpha + X_w\beta}{R_w^2+X_w^2} \tag{17}$$

$$\mu_r' = \frac{c}{\omega}\frac{R_w\beta + X_w\alpha}{Z_0} \tag{18}$$

and

$$\mu_r'' = \frac{c}{\omega}\frac{R_w\alpha - X_w\beta}{Z_0}. \tag{19}$$

### C. Genetic Algorithm for Material Properties Extraction

The constitutive parameters $\varepsilon_r(\omega)$ and $\mu_r(\omega)$ of a ferrite material are complex and frequency dependent. They can be approximated as a series of Debye-like terms (with poles of the first order) as [22]

$$\varepsilon_r(\omega) = \varepsilon_\infty + \sum_{p=1}^{P}\frac{\varepsilon_{sp}-\varepsilon_\infty}{1+j\omega\tau_p^e} + \frac{\sigma_e}{j\omega\varepsilon_0} \tag{20}$$

and

$$\mu_r(\omega) = 1 + \sum_{p=1}^{P}\frac{\chi_{sp}}{1+j\omega\tau_p^h}. \tag{21}$$

The parameters of these Debye-like terms $\varepsilon_{sp}, \varepsilon_\infty, \chi_{sp}, \tau_p^e, \sigma_e$, and $\tau_p^h$ can be extracted using a curve-fitting algorithm. In this paper, a GA has been adopted due to its robustness and global-search optimization nature [24], [25]. GAs are based on the mechanics of natural selection and genetics. The GA only needs to evaluate the objective function to guide its search, and there is no requirement for derivatives or other auxiliary knowledge. To implement a GA for solving an optimization problem, it is necessary to formulate the problem mathematically by defining an objective function, building up an analytic model, and choosing GA operators, such as selection, recombination, and mutation. Fig. 3(a)–(d) shows the measured complex permittivity and permeability frequency dependencies and the corresponding curves fitted using the GA.

The objective function for optimization for both permittivity and permeability is calculated through the mean-squared values with respect to all $N$ frequency points in the range of measurements. In the formulations for $\Delta\varepsilon$ and $\Delta\mu$

$$\Delta\varepsilon = \frac{1}{N}\sqrt{\sum_{i=1}^{N}\left\{\left(\frac{|\varepsilon_m'(f_i)-\varepsilon_e'(f_i)|}{\max|\varepsilon_m'(f_i)|}\right)^2+\left(\frac{|\varepsilon_m''(f_i)-\varepsilon_e''(f_i)|}{\max|\varepsilon_m''(f_i)|}\right)^2\right\}} \tag{22}$$

and

$$\Delta\mu = \frac{1}{N}\sqrt{\sum_{i=1}^{N}\left\{\left(\frac{|\mu_m'(f_i)-\mu_e'(f_i)|}{\max|\mu_m'(f_i)|}\right)^2+\left(\frac{|\mu_m''(f_i)-\mu_e''(f_i)|}{\max|\mu_m''(f_i)|}\right)^2\right\}} \tag{23}$$

the normalized deviation between the measured (subscript "$m$") and evaluated (subscript "$e$") values are considered. Fitness indices

$$P_\varepsilon = (\Delta\varepsilon)^{-0.33} \quad \text{and} \quad P_\mu = (\Delta\mu)^{-0.33} \tag{24}$$

are assigned to each set of parameters at each iteration cycle of the GA. They have been chosen empirically by numerous tests [26]. This index shows compatibility of each set with the other sets of data in the solution pool. A set with a higher index is allowed to have new offspring. The higher is $P_{\varepsilon,\mu}$, the closer the set to the solution.

Table I gives the extracted parameters for the DDM model, using the GA technique for the ferrite material of the magnetic core that was studied in the measurements. The frequency characteristics of permittivity of this particular material were approximated with two Debye terms and a low-frequency ohmic conductivity term, containing $\sigma_e$, and permeability was approximated with three Debye-like terms, one of which is negative. The negative term resulting form the curve fitting is a mathematical result rather than physical, and for this reason, we call them "Debye-like terms" rather than "Debye terms." Such negative terms still satisfy Kramers–Kronig causality relations.

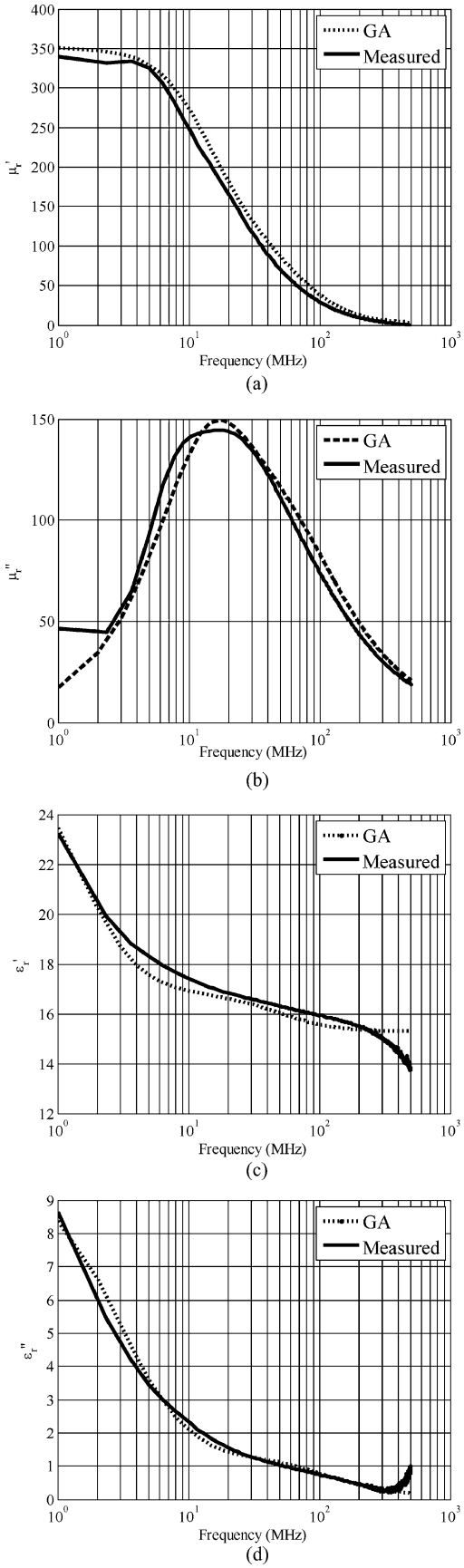


Fig. 3. Measured and GA extracted Debye curves: (a) real permeability, (b) imaginary permeability, (c) real permittivity, and (d) imaginary permittivity.

TABLE I
PARAMETERS OF THE DOUBLE-DEBYE MODEL

| | | | |
|---|---|---|---|
| $\varepsilon_\infty$ | 15.271 | $\mu_\infty$ | 1 |
| $\varepsilon_{s1}$ | 24.835 | $\mu_{s1}$ | 271.227 |
| $\varepsilon_{s2}$ | 16.75 | $\mu_{s2}$ | 104.46 |
| $\varepsilon_{s3}$ | - | $\mu_{s3}$ | -22.282 |
| $\tau_1^e$ (s) | $1.042\cdot10^{-7}$ | $\tau_1^h$ (s) | $1.149\cdot10^{-8}$ |
| $\tau_2^e$ (s) | $3.168\cdot10^{-9}$ | $\tau_2^h$ (s) | $2.364\cdot10^{-9}$ |
| $\tau_3^e$ (s) | - | $\tau_3^h$ (s) | $2.532\cdot10^{-8}$ |
| $\sigma_e$ (S/m) | $2.206\cdot10^{-4}$ | $\sigma_h$ (Ohm/m) | 0 |

### *D. Numerical Modeling of a Double-Debye Material Using FDTD Technique*

Representation of the frequency-dispersive permeability and permittivity of a magneto-dielectric (ferrite) material as a sum of Debye-like terms allows for implementing this material in numerical electromagnetic codes. The auxiliary differential equation (ADE) approach to treat complex frequency dependencies of constitutive parameters of materials is simple and efficient as compared to the other possible FDTD algorithms for treating dispersive materials, such as the recursive convolution (RC) [27], [28], the piecewise linear RC [28], [29], and the $Z$-transform method [30]. The ADE method [28], [31] uses duality for $E$ and $H$ fields, for auxiliary magnetic $M$ and electric $J$ sources, permittivity $\varepsilon$ and permeability $\mu$, and this makes this method comparatively simple for implementation in codes. The updating equations for the fields can be found in [32].

## III. COMPARISON BETWEEN SIMULATION AND MEASUREMENTS

The input impedances in short-circuit and open-circuit cases have been measured using an IA, and complex permittivity and permeability were extracted as described in Section II. The extracted functions $\mu_r'(f)$, $\mu_r''(f)$, $\varepsilon_r'(f)$, and $\varepsilon_r''(f)$ were approximated by Debye-like terms, using the GA. Then these data were used in the FDTD modeling of the same structure as was available in the measurements [33].

Fig. 4 shows the setup of the structure with a ferrite core for an FDTD model. The inner conductor has a radius $r_0$ of 3.6 mm, and the radius of the outer conductor is $r_1 = 7$ mm. The right part of the structure in Fig. 4(a) is the ferrite modeled as the DDM. The core has a length of 28 mm. In this model, to simulate infinitely long conductors and provide the TEM mode propagation in the modeled structure, the conductors are extended to touch the perfectly matched layer FDTD absorbing boundary on the left computational boundary (cross section A). The source of excitation (cross section B) was placed away from the actual input end (which is cross section D), at a distance of twice the length of the actual core. This was done only to numerically launch TEM/quasi-TEM mode waves through the

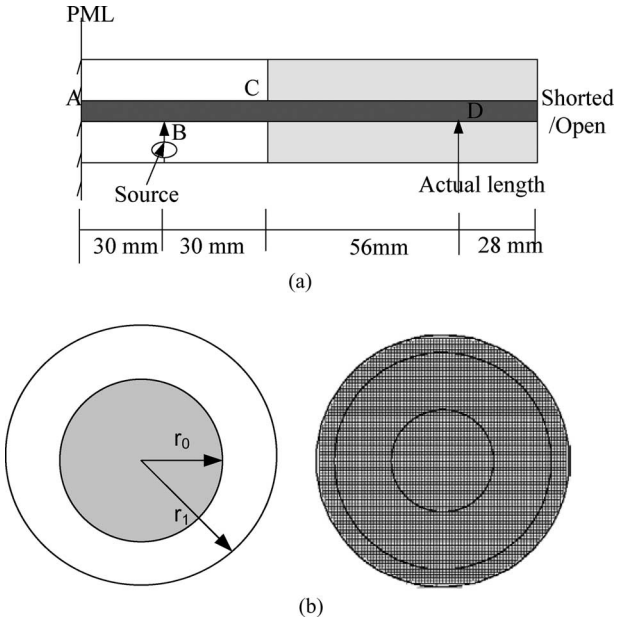


Fig. 4. Cross section of a magnetic core: (a) side view and (b) meshed cross section for the FDTD modeling.

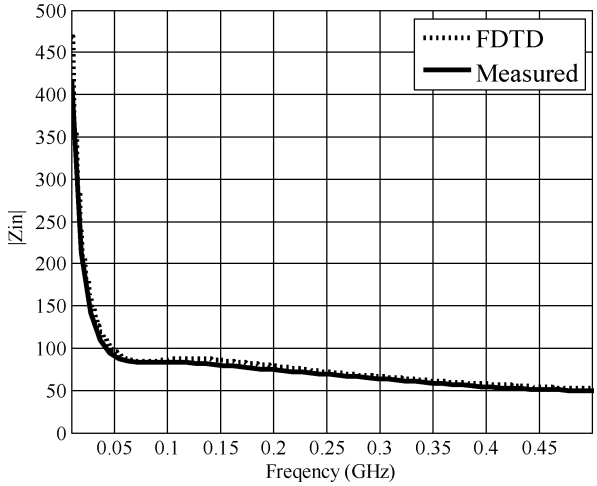


Fig. 5. FDTD modeled and measured input impedance of the ferrite core in the open-circuit case.

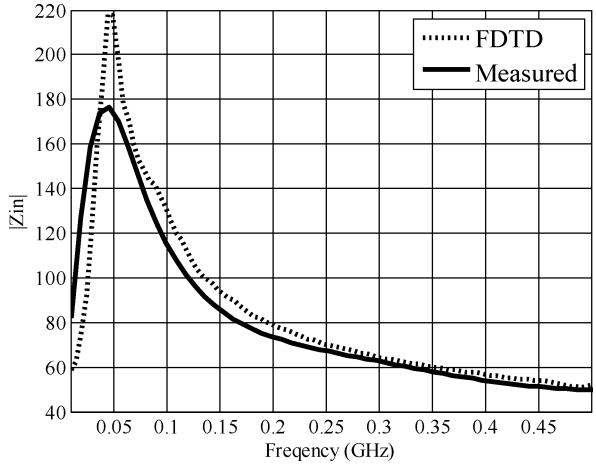


Fig. 6. FDTD modeled and measured input impedance of the ferrite core in the short-circuit case.

core. The ferrite core was also extended, as Fig. 3 shows, from the actual cross section D to the cross section C, which now is an interface between the ferrite and air. This was done to have reflections only from the shorted or open end of the core, and to avoid reflections from its other end. Since the ferrite material has a substantial loss, reflected waves from the interface of air and auxiliary part of the same material would attenuate and not interfere with the incident TEM wave. As soon as identical excitation of the ferrite core in the cross section D is provided in measurements and in simulations, then it does not matter what stands *before* this ferrite core.

The FDTD modeling uses only a rectangular mesh, so the circular cross-sectional geometry was approximated by a staircase grid with a cell size 0.4 mm in all three directions ($x$, $y$, and $z$), and the time step of 0.69 ps was chosen to satisfy the Courant stability limit.

Fig. 5 shows the simulation result together with the measured data for the open-circuit case, and good agreement between simulation and measurement is obtained over the entire frequency range from 10 to 500 MHz.

Fig. 6 shows the simulation results together with the measured data for the short-circuit termination. As seen in this figure, the agreement between the simulation and measured results in the short-circuit case is satisfactory, but it is not as good as that in the open circuit. The discrepancy between measured and simulated curves in both open- and short-circuit cases is due to a few factors. First, the actual geometry of the measured cylindrical core deviates from a perfect cylinder due to the manufacturing, it is somewhat conical, and there is no pure TEM wave in the measurements. At the same time, TEM mode propagation is forced in the simulations as described earlier. Second, a rectangular mesh is used to approximate a circular geometry. Third, some discrepancy is caused by lack of permittivity and permeability measurement points at lower frequencies in logarithmic frequency scale. Fourth, there might be some violation of Kramers–Kronig relations in measured frequency dependencies due to the accuracy of measurements. And finally, there is an approximation error when using the GA for curve fitting the ferrite's constitutive parameters. All these factors affect agreement for short-circuit termination much more than for the open circuit, since resonance effects are more pronounced in the short-circuit case due to stronger reflections.

Another ferrite-containing structure under test is shown in Fig. 7. This structure contains a 10-cm-long wire (24AWG) going through a rectangular ferrite block. The width A of the ferrite is 8 mm, the height D is 2.7 mm, and the length C is 12 mm. The height and width of the inner hollow hole are 0.9 and 6 mm, respectively. For the 10-cm-length wire, each leg has a length of 4 cm and the height is 2 cm.

In Fig. 8, the input resistance and reactance versus frequency from 10 MHz to 1.8 GHz are shown. Over the lower frequency range from 10 to 500 MHz, the curves of input reactance match

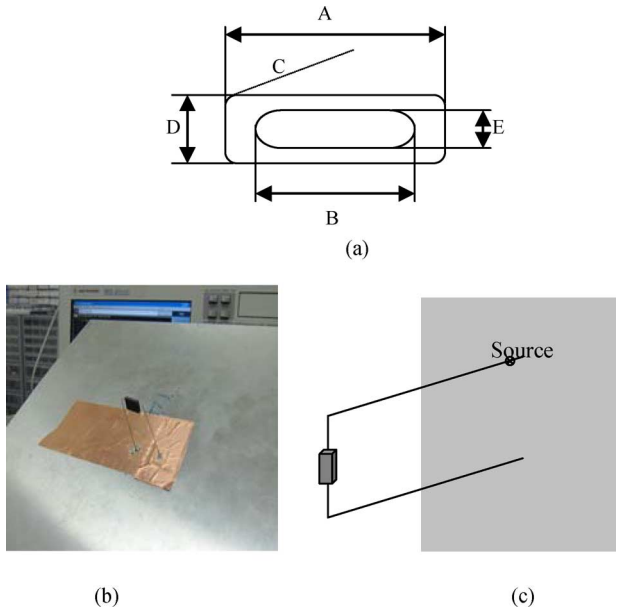


Fig. 7. Geometry of a ferrite block: (a) cross-sectional view; (b) setup of measurement; and (c) simulation model.

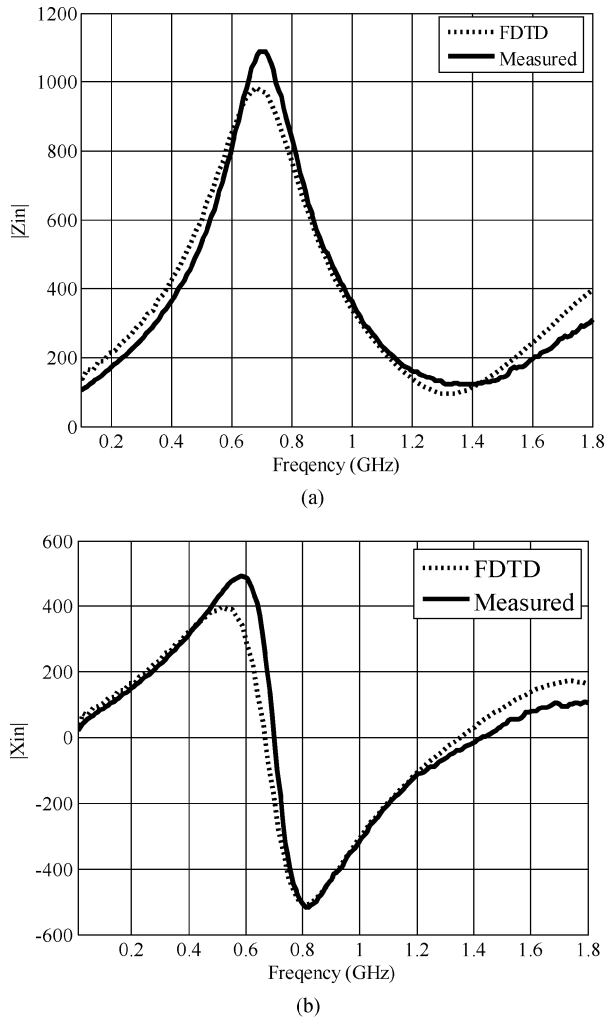


Fig. 8. FDTD modeled and measured input impedance of the 10 cm wire together with a ferrite block: (a) input impedance. (b) reactance.

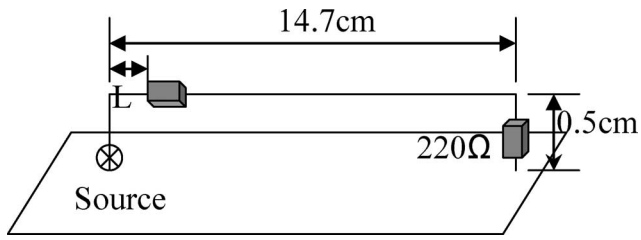


Fig. 9. Geometry of the 14.7 cm transmission line: (a) setup of measurement and (b) simulation model.

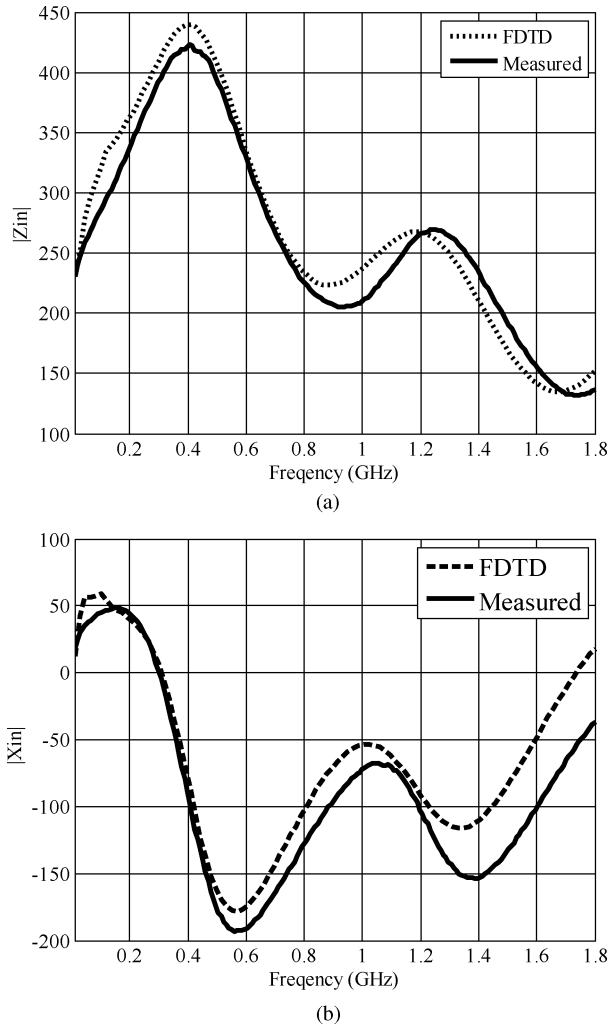


Fig. 10. FDTD modeled and measured input reactance for the 15 cm wire together with a ferrite block: (a) input impedance. (b) reactance.

very well. For the input resistance, the difference between these two curves is due to the perfect electric conductor assumption for the thin-wire model in FDTD. Note also that resonant frequencies are matching.

However, it was observed in the earlier example that the input impedance is dominated by the wire, but not the ferrite block. For this reason, it was important to design a new, more wideband test structure, which would allow for obtaining results that depend more on ferrite. Such test structure geometry is shown in Fig. 9. It is composed of a 14.7-cm length wire (24AWG)

at 0.5-cm distance above the ground plane. This transmission line is matched at the load side (220-Ohm termination resistor), and the matching quality is checked using time-domain reflectometer, which shows a flat response. Then the ferrite block (the same as in the previous case) is placed around the wire at the distance $L = 1$ cm from the source.

Fig. 10 shows the simulated and measured input resistance and reactance for the geometry, as shown in Fig. 9. The discrepancy between the measured and simulated results in different parts of the frequency range is mainly caused by the quality of curve fitting of real and imaginary parts of permittivity and permeability (see Fig. 3).

## IV. Conclusion

A practical and systematic approach for design of ferrite chokes has been proposed in this paper. Both permittivity and permeability of a ferrite material can be measured using a hollow cylindrical ferrite sample with silver-plated internal and external surfaces, representing a ferrite-filled coaxial-line structure. The measurement technique requires obtaining data for input impedances in short-circuit and open-circuit cases for this structure. In the example considered in this paper, the measurements were done for the frequency range from 10 to 500 MHz, using an IA, but the similar results can be obtained using a network analyzer. The extraction of dispersive dielectric and magnetic properties was done based on the transmission line theory and application of a GA.

Dielectric and magnetic properties of dispersive materials can be effectively extracted using the proposed method and the specially designed waveguiding structures with completely filled cross section. These may be not only coaxial lines, but striplines as well, provided that there is only TEM/quasi-TEM wave propagation.

The permittivity and permeability data obtained from measurements with a silver-coated ferrite hollow cylinder were then plugged into the EZ-FDTD codes to model the same cylinder. These codes treat dispersive magneto-dielectric materials as a "double-Debye material" using ADEs. It is shown that the obtained results for the input impedances in open- and short-circuit cases agree well.

Additional experimental and numerical testing was conducted on two structures containing a rectangular ferrite choke (block) made of the same ferrite material as the hollow cylindrical core. The satisfactory agreement between modeled and measured results serves as a validation for both the proposed material parameter extraction technique and the FDTD codes that can be used for expedited design of ferrite cores and other ferrite-containing structures needed for SI and EMC purposes.

## References


[1] P. Han, G. R. Skutt, J. Zhang, and F. C. Lee, "Finite element method for ferrite core loss calculations," in *Proc, 10th Appl. Power Electron. Conf.*, Mar. 5–9, 1995, vol. 1, pp. 348–553.

[2] K. V. Namjoshi, J. D. Lavers, and P. P. Biringer, "Eddy-current power loss in toroidal cores with rectangular cross section," *IEEE Trans. Magn.*, vol. 34, no. 3, pp. 636–641, May 1998.

[3] R. Huang and D. Zhang, "Using a single toroidal sample to determine the intrinsic complex permeability and permittivity of Mn-Zn ferrites," *IEEE Trans., Magn.*, vol. 43, no. 10, pp. 3807–3815, Oct. 2007.

[4] B. Lax and K. J. Button, *Microwave Ferrites and Ferrimagnetics*. New York: McGraw-Hill, 1962.

[5] D. Polder, "Ferrite materials," in *Proc. IEE- Inst. Electr. Eng.*, 1950, vol. 97, Part II, pp. 246–256.

[6] M. N. Afsar, K. Korolev, and L. Subramanian, "Complex permittivity and permeability measurements of ferrimagnets at millimeter waves with high power sources," *IEEE Tran. Magn.*, vol. 41, no. 10, pp. 3457–3459, Oct. 2005.

[7] K. A. Korolev, S. Chen, and M. N. Asfar, "Complex magnetic permeability and dielectric permittivity of ferrites in millimeter waves," *IEEE Trans. Magn.*, vol. 44, no. 4, pp. 435–437, Apr. 2008.

[8] G. T. Rado, "Magnetic spectra of ferrites," *Rev. Modern Phys.*, vol. 25, no. 1, pp. 81–89, Jan. 1953.

[9] E. B. Mullen and E. R. Carlson, "Permeability tensor values from waveguide measurements," in *Proc. IRE*, Oct. 1956, pp. 1318–1323.

[10] S. Sensiper, "Resonance loss properties of ferrites in 9 KMC region," in *Proc. IRE*, Oct. 1956, pp. 1323–1343.

[11] G. Roussy, H. Chaabane, and H. Esteban, "Permittivity and permeability measurement of microwave packaging materials," *IEEE Tran. Microw. Theory Tech.*, vol. 52, no. 3, pp. 903–907, Mar. 2004.

[12] J. Backer-Jarvis, R. Geyer, and P. Domich, "Improvement in transmission line permittivity and permeability measurements," in *Proc. CPEM1990 Digest, IEEE Conf. Precision Electromagn. Meas.*, 11–14 Jun. 1990, pp. 232–233.

[13] M. Ledieu and O. Acher, "New achievements in high-frequency permeability measurements of magnetic materials," *J. Magn. Magn. Mater.*, vol. 258–259, pp. 144–150, 2003.

[14] V. Bekker, K. Seemann, and H. Leise, "A new strip line broad-band measurement evaluation for determining the complex permeability of thin ferromagnetic films," *J. Magn. Magn. Mater.*, vol. 270, pp. 327–332, 2004.

[15] A. M. Nicolson and G. F. Ross, "Measurement of the intrinsic properties of materials by time-domain techniques," *IEEE Trans. Instrum. Measur.*, vol. 19, no. 4, pp. 377–382, Nov. 1970.

[16] R. Huang and D. Zhang, "Characterization of Mn-Zn ferrites using the coaxial transmission line method," *IEEE Trans. Magn.*, vol. 44, no. 7, pp. 1703–1710, Jul. 2008.

[17] W. Weir, "Automated measurement of complex dielectric constant and permeability at microwave frequencies," *Proc. IEEE*, vol. 62, no. 1, pp. 33–36, Jan. 1974.

[18] W. Barry, "A broadband automated stripline technique for simultaneous measurement of complex permittivity and permeability," *IEEE Trans. Microw. Theory Techn.*, vol. MTT-34, no. 1, pp. 80–84, Jan. 1986.

[19] J. Hu, A. Sligar, C. Chang, S. Lu, and R. K. Settaluri, "A grounded coplanar waveguide technique for microwave measurement of complex permittivity and permeability," *IEEE Trans., Magn.*, vol. 42, no. 7, pp. 1929–1931, Jul. 2006.

[20] F. T. Ulaby, *Fundametals of Applied Electromagnetics*. 2004 Media Edition. Englewood Cliffs, NJ: Pearson Prentice-Hall, 2004, ch. 2–7, pp. 60–61.

[21] V. Lucarini, J. J. Saarinen, K.-E. Peiponen, and E. M. Vartiainen, *Kramers-Kronig Relations in Optical Materials Research*, vol. 110. New York: Springer Series in Optical Sciences, 2005.

[22] M. Y. Koledintseva, J. Wu, J. Zhang, J. L. Drewniak, and K. N. Rozanov, "Representation of permittivity for multi-phase dielectric mixtures in FDTD modeling," in *Proc. IEEE Symp. Electromag. Compat.*, Santa Clara, CA, 9–13 Aug. 2004, vol. 1, pp. 309–314.

[23] M. D. Janezic, D. F. Williams, V. Blaschke, A. Karamcheti, and Chi Shih Chang, "Permittivity characterization of low-k thin films from transmission-line measurements," *IEEE Trans. Microw. Theory Tech.*, vol. 51, no. 1, p. 132- 136, Jan. 2003.

[24] R. L. Haupt, "An introduction to genetic algorithms for electromagnetics," *IEEE Trans. Antennas Propag.*, vol. 37, no. 2, pp. 7–15, Apr. 1995.

[25] J. Zhang, M. Koledintseva, J. Drewniak, D. Pommerenke, R. DuBroff, Z. Yang, W. Cheng, G. Antonini, and A. Orlandi, "Reconstruction of dispersive dielectric properties for PCB substrates using a genetic algorithm," *IEEE Trans. Electromag. Compat.*, vol. 50, no. 3, pp. 704–714, Aug. 2008.

[26] J. Zhang, M. Y. Koledintseva, D. J. Pommerenke, J. L. Drewniak, K. N. Rozanov, G. Antonini, and A. Orlandi, "Extraction of dielectric material

parameters for dispersive substrates using a genetic algorithm," in *Proc. 2006 IEEE Instrum. Meas. Technol. Conf. (IMTC)*, Sorrento, Italy, Apr. 24–27, 2006, pp. 462–467.

[27] K. S. Kunz and R. J. Luebbers, *The Finite Difference Time Domain Method for Electromagnetics*. Boca Raton, FL: CRC Press, 1993.

[28] A. Taflove and S. C. Hagness, *Computational Electrodynamics: The Finite-Difference Time-Domain Method*, 3rd ed. Norwood, MA: Artech House, 2005.

[29] D. K. Kelley and R. J. Luebbers, "Piecewise linear recursive convolution for dispersive media using FDTD," *IEEE Trans. Antennas Propag.*, vol. 44, no. 6, pp. 792–792, Jun. 1996.

[30] D. M. Sullivan, "Frequency-dependent FDTD methods using Z transforms," *IEEE Trans. Antennas Propag.*, vol. 40, no. 10, pp. 1223–1230, Oct. 1992.

[31] S. Kong, J. Simpson, and V. Backman, "ADE-FDTD scattered-field formulation for dispersive materials," *IEEE Microw. Wireless Commun. Lett.*, vol. 18, no. 1, pp. 4–6, Jan. 2008.

[32] M. Koledintseva, J. Drewniak, Y. Zhang, J. Lenn, and M. Thoms, "Engineering of ferrite-based composite materials for shielding enclosures," *J. Magn. Magn. Mater.*, vol. 321, pp. 730–733, Mar. 2009.

[33] J. Xu, M. Y. Koledinstseva, Y. He, R. E. DuBroff, J. L. Drewniak, and B. Matlin, "Measurement of electromagnetic parameters and FDTD modeling of ferrite cores," in *Proc. IEEE Symp. Electromag. Compat.*, Austin, TX, Aug. 2009, pp. 83–88.

**Jianfeng Xu** (M'08) received the Ph.D. degree in electronic engineering from Shanghai Jiao Tong University, Shanghai, China, in 2007

He is currently a Researcher in the Electromagnetic Compatibility Laboratory, University of Missouri Science and Technique, Rolla. His research interests include computational electromagnetics.

**Marina Y. Koledintseva** (M'96–SM'03) received the M.S. degree (highest honors) and the Ph.D. degree, in 1984 and 1996, respectively, from the Radio Engineering Department of Moscow Power Engineering Institute (Technical University) (MPEI(TU)), Moscow, Russia.

From 1983 to 1999, she was a Researcher with the Ferrite Laboratory, MPEI (TU), where she was an Associate Professor from 1997 to 1999. In January 2000, she was a Visiting Professor and has been with the Electromagnetic Compatibility (EMC) Laboratory, University of Missouri-Rolla, which became Missouri University of Science and Technology (MS&T), Rolla since 2008. Since 2005, she has been a Research Professor in MS&T. She is the author or coauthor of about 150 papers. She holds seven patents. Her scientific interests include microwave engineering, interaction of electromagnetic field with ferrites and composite media, their modeling, and application for electromagnetic compatibility.

Prof. Koledintseva is a member of the Education, TC-9 Computational Electromagnetics, and TC-11 (Nanotechnology) Committees of the IEEE Electromagnetic Compatibility Society.

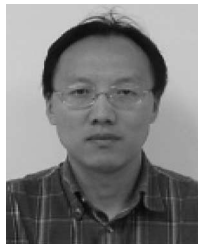

**Yaojiang Zhang** (M'01) received the B.E. and M.E. degrees in electrical engineering from the University of Science and Technology of China, Hefei, China, in 1991 and 1994, respectively, and the Ph.D. degree in physical electronics from Peking University, Beijing, China, in 1999.

From 1999 to 2001, he was with Tsinghua University, Beijing, China, as a Postdoctoral Research Fellow. From August 2001 to August 2006, he was a Senior Research Engineer in the Institute of High Performance Computing (IHPC), Agency for Science, Technology and Research (A∗STAR), Singapore. From September 2006 to September 2008, he was a Postdoctoral Research Fellow in the Electromagnetic Compatibility Laboratory (EMC Lab), Missouri University of Science and Technology (formerly University of Missouri-Rolla), Rolla. From September 2008 to April 2010, he was with the Computational Electronics and Photonics, IHPC. He is currently a Research Associate Professor in the EMC Lab. His research interests include computational electromagnetics, parallel computing techniques, and signal integrity and power integrity issues in high-speed electronic packages or printed circuit boards.

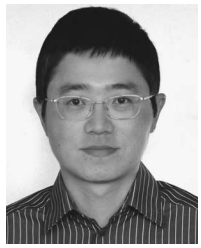

**Yongxue He** received the B.S. degree in applied physics, the M.S. degree in optics, both from Tsinghua University, Beijing, China, and the Ph.D. degree in EE from Northeastern University, Boston, MA.

He is currently an RF Engineer at Laird Technologies, Chattanooga, TN. He is an expert in signal integrity components, electromagnetic interference shielding, and microwave absorber.

**Bill Matlin** received the B.S.M.E. degree from Vanderbilt University, Nashville, TN, in 1986, and the M.S. degree in material science from the University of Tennessee, Knoxville, TN, in 1995.

Since 2002, he has been with Laird Technologies, Chattanooga, TN, where he is currently the Director of Technology for the Signal Integrity Business Unit. He has held materials development positions and engaged in research on super-alloys, silicon wafers, and soft ferrites.

**Richard E. DuBroff** (S'74–M'77–SM'84) received the B.S.E.E. degree from Rensselaer Polytechnic Institute, Troy, NY, in 1970, and the M.S. and Ph.D. degrees in electrical engineering from the University of Illinois, Urbana-Champaign, in 1972 and 1976, respectively.

From 1976 to 1978, he was a Postdoctoral Researcher in the Ionosphere Radio Laboratory, University of Illinois, where he was engaged in research on backscatter inversion of ionospheric electron density profiles. From 1978 to 1984, he was a Research Engineer in the geophysics branch of Phillips Petroleum, Bartlesville, OK. Since 1984, he has been with the University of Missouri-Rolla, Rolla (renamed as the Missouri University of Science and Technology in 2008), where he is currently a Professor in the Department of Electrical and Computer Engineering and the Director of the Electromagnetic Compatibility Laboratory, and where he has served as an Associate Chairman for graduate studies from 1991 to 1996 and from 2002 to 2009.

**James L. Drewniak** (S'85–M'90–SM'01–F'06) received the B.S., M.S., and Ph.D. degrees in electrical engineering from the University of Illinois, Urbana-Champaign, in 1985, 1987, and 1991, respectively.

In 1991, he joined the Electrical and Computer Engineering Department, University of Missouri-Rolla (presently Missouri University of Science and Technology, Rolla), where he has been one of the principal investigators in the Electromagnetic Compatibility (EMC) Laboratory and a Full-Professor in the Electrical and Computer Engineering Department. From 2002 to 2007, he was the Director of the Materials Research Center, University of Missouri-Rolla. His current research interests include EMC in high-speed digital and mixed signal designs, electronic packaging, *microelectromechanical systems*, EMC in power electronic-based systems, and numerical modeling for EMC applications.

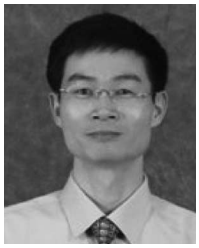

**Jianmin Zhang** (S'02–M'07–SM'09) received the B.S. degree from the Southeast University, Nanjing, China, in 1985, and the M.S. and Ph.D. degrees in electrical engineering from the University of Missouri-Rolla, Rolla (renamed as Missouri University of Science and Technology in 2008), in 2003 and 2007, respectively.

He was with Nanjing Electronic Equipment Research Institute, China, as a Hardware Engineer for more than ten years. In 2007, he joined Cisco Systems, San Jose, CA, as a Senior Hardware Engineer, where he is currently engaged in research on signal integrity and power integrity R&D for high-speed interconnects and is involving in design and analysis for high-performance networking products at printed circuit board (PCB), package, and system levels. He is the author or coauthor of more than 40 technical papers and presentations. He holds three issued patents in China. His research interests include signal integrity, power integrity, SerDes modeling, electromagnetic interference/electromagnetic compatibility (EMC), and PCB material characterization for high-speed digital systems.

Dr. Zhang is the Technical Committee Member of DesignCon 2009, 2010, and 2011, and the organizer of Track 13. He is the member of TC-9 and TC-10 of the IEEE EMC Society and a member of the International Reviewer's Board for EMC Europe 2008 and 2010. He is also a Reviewer for a number of international conferences and two journals. He was the recipient of the Best Symposium Paper Award and the Best Student Symposium Paper Award from the IEEE EMC Society in 2006, and the Conference Best Session Paper Award in signal integrity from the International Microelectronics and Packaging Society in 2007.